Acta Technica 62, No. 1A/2017, 11–20

The damage effect of explosions on immersed tube cross-river tunnels

Yin Ni[1,2], Yonglai Zheng[1], Fang Li[1]

Abstract. Taking Shanghai Outer Ring Tunnel as an example, the safety of immersed tube cross-river tunnels under air defense loads is studied. Using the finite difference software FLAC, a model is built according to the coefficient of subgrade reaction derived from a dynamic triaxial test. The internal force distribution of a typical cross section in the main structure of tunnel under different working conditions is calculated. The joint opening of the immersed tube caused by longitudinal differential settlement under air defense loads is calculated, too. Results show that setting protective doors in a tunnel can significantly improve the blastproof performance of the immersed tube structure and keep the joint displacement of differential settlement within a controllable range.

Key words. Immersed tube tunnel, explosive effect, protective door, resistance coefficient, longitudinal settlement.

1. Introduction

At present, there are many lessons and theories about earthquake resistance and hazard reduction of cross-river tunnels at home and abroad. A vast majority of them focus on tunnels constructed with the advanced shield tunneling method today. But few are reported on the air defense of immersed tube tunnels. Cross-river tunnels, as key nodes of urban traffic trunks, used to be air defense evacuation exits and temporary shelters during wars. So they must be able to resist nuclear explosions in the wartime. Liu Ganbin et al. [1] carried out a numerical simulation on dynamic response of tunnels in soft soil under explosive loads and gave the dynamic response law of nodes in particular parts. Chen Bin et al. [2] studied the explosive shock wave load on a cross-river tunnel for metro. Lu Zhifang [3] analyzed dynamic response and damage of Yangtze River Tunnel under different explosive loads. Shi Xianwei [4] studied the structural calculation and analysis on an immersed tube cross-river tunnel from Yuzhu Wharf, Guangzhou to Changzhou Island and concluded that the greater difference between adjacent coefficients of subgrade reaction, the greater

[1]Department of Civil Engineering, Tongji University, Shanghai, 200092, China
[2]China State Construction Harbour Construction Co., LTD, Shanghai, 201300, China

negative bending moment peak. One of our research team members, Xiao Li et al. [5] examined the damage effect of a nuclear explosion on a cross-river shield tunnel and reported that setting protective doors in the shield tunnel can effectively prevent the effect of nuclear explosive shock wave on the structure of tunnel.

Different construction processes between immersed tube tunnel and shield tunnel also lead to different structural performances. The immersed tube tunnel adopts a reinforced concrete rectangular framework. There is multifarious equipment in the tunnel. It remains a controversy whether a protective airtight door needs to be set in the immersed tube tunnel. Therefore, it is necessary to study the damage effect of explosive load on immersed tube tunnels and identify the importance of protective airtight doors.

2. State of the art

Outer Ring Tunnel is the last single construction project along Shanghai outer ring. It is about 2000 m away from Wusong Port and 2880 m in length. Being the first cross-river tunnel constructed with immersed tube in Shanghai, Outer Ring Tunnel is composed of seven immersed tubes, each of which is equivalent to more than half of a soccer field. After drainage, leakage detection and other procedures, the immersed tubes are floated and transported to water surface and gradually sunk to desired positions. After tested, facilities on the end faces of segments are dismantled and assembled in water as a whole. Sand is filled between the tube bottom and riverbed by pressure to form foundations of segments. E7 and E6 segments are sunk into Pudong, while E1 to E5 segments are sunk into Puxi in proper order. Finally, E5 and E6 segments are jointed, to make the tunnel run-through as a whole [6].

E4 segment in the river is taken as a typical cross section, as shown in Fig. 1. E4 segment is a prefabricated immersed tube, whose cross section is 43 m wide and 9.55 m high. The lining of roof is 1.5 m thick. The side wall is 1.0 m thick. The floor is 1.5 m thick. The interior wall is 0.55 m thick. Roadway slabs are connected with the entire structure and filled with C30 concrete [6].

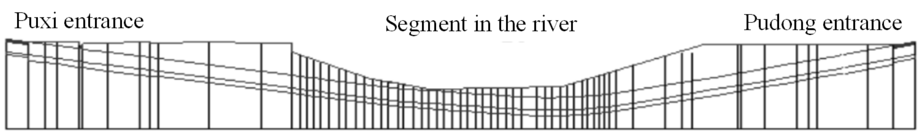

Fig. 1. Longitudinal section of outer ring tunnel

3. Methodology

Air defense loads can be divided into two working conditions, Grade-6 nuclear weapon and Grade-6 conventional weapon. For some of the parameters, we suppose as follows:

Suppose that all layers have the same soil parameters, i.e., the soil is a single soil medium, whose properties are shown in Table 1.

Table 1. Properties of soil layers

Soil/Structure	Density (kg/m^3)	Elasticity modulus	Poisson's ratio	Bulk modulus	Shear modulus
Clayey silt	1860	3.471×10^7	0.30	2.892×10^7	1.335×10^7
Silty clay	1870	2.390×10^7	0.30	1.992×10^7	9.192×10^6
Mucky clay	1780	2.390×10^7	0.30	1.992×10^7	9.192×10^6
Backfill	1862	5.849×10^6	0.31	5.173×10^6	2.23×10^6
Huangpu River silt	1700	2.501×10^6	0.20	1.389×10^6	1.042×10^6

Under a nuclear explosion, when air shock wave propagates inside the tunnel, shock wave attenuation caused by energy loss incurred in the propagation process is ruled out. Meanwhile, it is supposed that the impact of tunnel shape transformation has little impact on shock wave parameters. Relevant factors can be neglected.

The impact of river water on shock wave in the propagation process is ruled out, i.e., it is believed that shock wave does not attenuate when propagating in water. When calculating the impact of conventional weapon, we rule out the impact of river water, too.

Under a nuclear explosion, given the short duration of shock wave, the internal air shock wave and external compression wave from soil are not applied to the structure simultaneously when calculating.

The overpressure of straight-in internal shock wave inside the structure is equal to the overpressure of ground shock wave ΔP_{m}. The overpressure of superimposed internal shock wave is three times as large as the overpressure of ground shock wave $3\Delta P_{\mathrm{m}}$ [7].

According to a dynamic triaxial test conducted by our team on undisturbed soil [5] and [8], the coefficient of subgrade reaction is calculated. The silty clay is $5130\,\mathrm{kN/m^3}$. The clayey silt is $4510\,\mathrm{kN/m^3}$. The silt and backfill is $2080\,\mathrm{kN/m^3}$.

For nuclear explosion, the waveform of compression wave in soil is simplified into a triangle of pressure rise time. The maximum pressure and pressure rise time can be calculated as

$$p_{\mathrm{h}} = [1 - \frac{h}{c_1 t_2}(1-\delta)]\Delta P_{\mathrm{m}}\,, \tag{1}$$

$$t_{0\mathrm{h}} = (\gamma - 1)\,\frac{h}{\nu_0}\,, \tag{2}$$

and

$$\gamma = \frac{\nu_0}{\nu_1}\,, \tag{3}$$

where p_{h} (MPa) is the pressure peak of compression wave. Symbol ΔP_{m} (MPa) is the overpressure peak of ground air shock wave and h (m) is the calculation depth of soil. When calculating roof, the thickness of covering soil is adopted. Symbol $t_{0\mathrm{h}}$

(s) is the pressure rise time of compression wave and t_2 (s) is the pressure drop time. Finally, δ is the residual strain ratio of soil, γ is the velocity ratio, ν_0 (m/s) is the initial pressure velocity of the soil and ν_1 (m/s) is the peak pressure velocity of the soil.

For the impact of an indirect hit of conventional weapon on the structure, we assume that under a Grade-6 air defense, with the increase of distance from charging point, explosive loads on different positions decrease. The resulting pressure peak of compression wave can be calculated as [9]

$$\Delta P_{\mathrm{m}} = 1.316 \left(\frac{L_{\mathrm{i}}}{\sqrt[3]{C}} \right)^{-3} + 0.369 \left(\frac{L_{\mathrm{i}}}{\sqrt[3]{C}} \right)^{-1.5}, \tag{4}$$

$$p_{\mathrm{h}} = \Delta P_{\mathrm{m}} \exp \left(-n_1 \sqrt[3]{\frac{h}{1000\tau_i}}, \right) \tag{5}$$

where ΔP_{m} (MPa) is the overpressure peak of ground shock wave at the projection point of slab center on the earth's surface. Symbol L_{i} denotes the horizontal distance from the charging center to calculation point, and C is the equivalent TNT load of conventional weapon. Finally, n_1 is the attenuation coefficient in soil and τ_i (s) is the duration of overpressure.

Equivalent static load method is used for calculation. According to resistance standards to Grade-6 nuclear explosion and Grade-6 conventional weapon, using a three-coefficient method, standard values are adopted for the roof equivalent static load, side wall equivalent static load and floor equivalent static load of the tunnel respectively [9].

4. Result analysis and discussion

4.1. Modeling

When protective air-tight doors are set on the entrances on both sides of the cross-river tunnel, a nuclear explosive shock wave acts on the external structure, known as external shock wave effect. If protective doors are not set in a timely manner, shock wave will rush into the tunnel from the entrances and produce a superimposed shock wave effect in the middle of tunnel (in the river). In Fig. 2, P_{roof} is the load of covering soil, P_{bottom} is the subgrade reaction, P_1 and P_2 are pressures from top and lateral soil, P_ν is the load of vehicle, P_{n1}, P_{n2} and P_{n3} are air defense loads on the roof, side wall and floor. Further, P_{in} is the internal shock wave load. Among them, pressures from covering soil and lateral soil, as well as gravity load are calculated using a soil mechanics approach.

Under an explosive load, standard values of the uniform equivalent loads on the roof, side wall and floor of the immersed tube can be calculated as

$$P_{\mathrm{n1}} = K_{\mathrm{d1}} \cdot K \cdot P_{\mathrm{h}}, \tag{6}$$

$$P_{\mathrm{n2}} = K_{\mathrm{d2}} \cdot \zeta \cdot P_{\mathrm{h}}\,, \tag{7}$$

$$P_{\mathrm{n3}} = K_{\mathrm{d3}} \cdot \eta \cdot P_{\mathrm{h}}\,, \tag{8}$$

where K_{d1}, K_{d2} and K_{d3} are dynamic coefficients of the roof, side wall and floor, K is the comprehensive reflection coefficient of roof, ζ stands for the pressure from lateral soil, and η is pressure from bottom soil. The specific values are shown in [9].

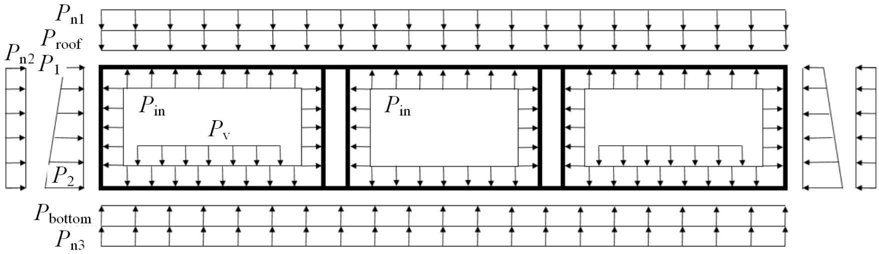

Fig. 2. Calculation model of E4 segment

Considering that E4 segment lies in the river and involves three working conditions, i.e., mean high water level, mean low water level and highest navigable water level, the water level elevation in its location can be divided into 1.02 m mean low water level (Huangpu River Elevation System, similarly hereinafter), 3.25 m means the high water level and 5.99 m is the highest navigable water level [10]. The most unfavorable conditions are adopted.

Using general finite element software FLAC5.0, the internal static force of plane strain is calculated. Using the Beam element structure in Struct module, the framework, roadway slab and internal partition of the tube are simulated. Beam elements of the rectangular framework are connected with stiff joints. The internal partition and framework are also connected with stiff joints. In FLAC5.0, beam elements can only add normal and tangential loads, so the loads are simplified into concentrated loads on nodes. Beam elements are 1.0 m wide, in order to reduce the calculation error. For ease of calculation, this rectangular tunnel is divided into 8 beam elements, which move in the horizontal restraint direction X and vertical restraint direction Y on the bottom left and right of the structure. The calculation model of FLAC is shown in Fig. 3.

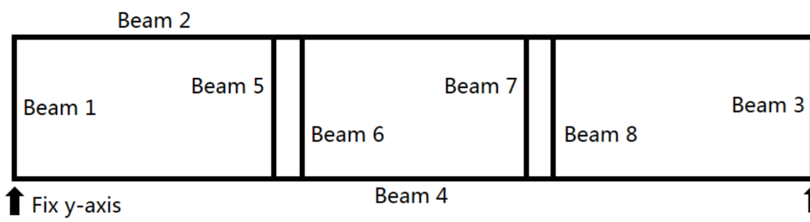

Fig. 3. Calculation model of FLAC

Beam 1 is the left wall in the left channel, beam 2 is the roof, beam 3 is the right wall in right channel, beam 4 is the floor, beam 5 is the right wall in left channel, beam 6 is the left wall in middle channel, beam 7 is the right wall in middle channel, and beam 8 is the left wall in the right channel.

4.2. Calculation results

Under a Grade-6 nuclear explosion, with protective doors, the internal force effects on cross section are depicted in Figs. 4 and 5.

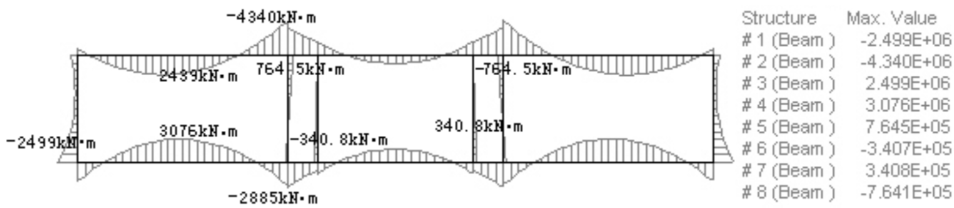

Fig. 4. Bending moment diagram (Grade-6, nuclear explosion, with protective doors

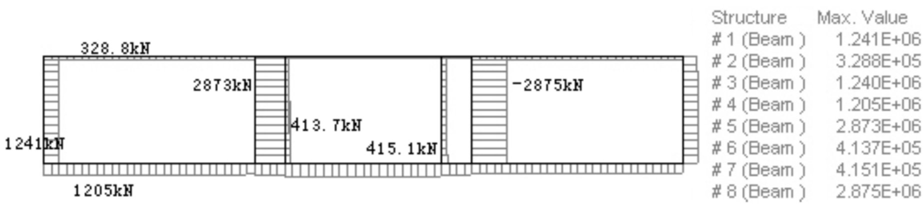

Fig. 5. Axial force diagram (Grade-6, nuclear explosion, with protective doors

Under a Grade-6 nuclear explosion, without protective doors, the internal force effects of superimposed shock wave on cross section are depicted in Figs. 6 and 7.

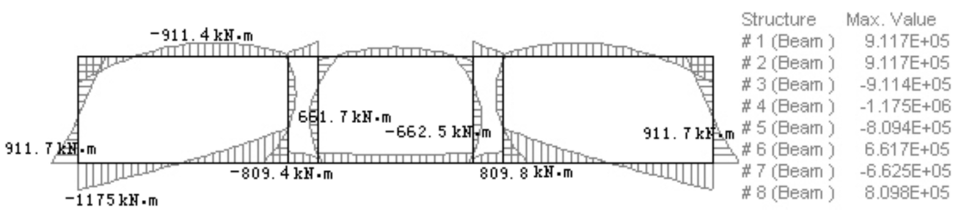

Fig. 6. Bending moment diagram (Grade-6, nuclear explosion, with protective doors open

4.3. Internal force analysis

Under the impact of a dynamic load, the strength of structural material is improved to a certain extent. When calculating reinforcement, the strength of structural material is adjusted [9], as shown in Table 2 below.

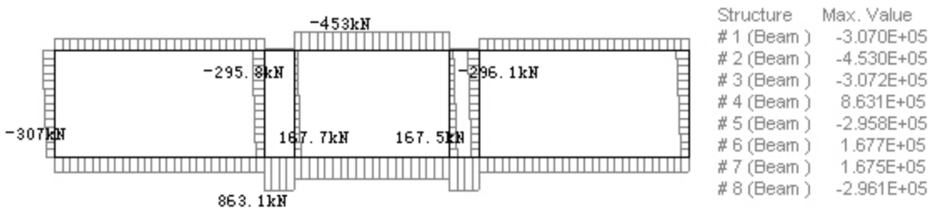

Fig. 7. Axial force diagram (Grade-6, nuclear explosion, with protective doors open

Table 2. Adjustment of material strength in dynamic calculation

Material	HPB235	HRB335	C30	C50
Strength before adjustment ((kN/m^2))	210	300	14.3	23.1
Strength after adjustment (kN/m^2)	315	405	19.305	31.185

Since the bending moment and axial force produced by an indirect hit of conventional weapon on the structure of an immersed tube tunnel with Grade-6 protection are far lower than the impact of nuclear explosion under the same conditions, in our study, when calculating reinforcement, we only calculate the effect of nuclear explosion. The calculation results are shown in Table 3. Under a Grade-6 nuclear explosion, with protective doors, all of the members of immersed tube satisfy requirements. Without protective doors, the right wall of left channel, left wall of right channel and left and right walls of middle channel do not meet the requirements for flexural capacity.

Table 3. Calculation results

Air defense grade	Member name	With protective doors	Without protective doors
Air defense grade	Roof (max positive bending moment)	Satisfied	Satisfied
	Roof (max negative bending moment)	Satisfied	Satisfied
	Right wall of right channel	Satisfied	Satisfied
	Floor (max positive bending moment)	Satisfied	Satisfied
	Floor (max negative bending moment)	Satisfied	Satisfied
	Right wall of left channel	Satisfied	Not satisfied
	Left wall of middle channel	Satisfied	Not satisfied
	Right wall of middle channel	Satisfied	Not satisfied
	Left wall of right channel	Satisfied	Not satisfied

4.4. Modeling calculation and analysis of longitudinal section

4.4.1. Modeling We consider differential settlement caused by Grade-6 nuclear explosion within 1600 m of the tunnel, with protective doors. Using the finite difference software FLAC, a longitudinal section model is built. Elastic models are adopted for the soil and tunnel structure. We make river water equivalent to hydrostatic pressures and load them to corresponding positions on the soil surface. Given that the existence of tunnel will not resist differential settlement under a dynamic weapon load, materials with the same properties as soil elements are used for the tunnel. The boundary conditions of model are: with the base fixed, move in the direction of Y and with left and right sides fixed, move in the direction of X.

Assume that protective doors are set on both ends of the tunnel. The shock wave load of Grade-6 nuclear explosion on the soil surface is 0.05 MPa and loaded on the model roof. Before loading, river water loads on corresponding positions of the model are calculated.

4.4.2. Calculation results The model is calculated using FLAC in two steps.

Step 1: to let the model reach an initial balance under acceleration of gravity, without a dynamic weapon load.

Step 2: to reset the displacement produced by the initial balance and add a weapon load, calculate until a balance is reached. Using detection points along the tunnel model, values of differential settlement at various points are recorded [11-12].

A curve fitting is conducted on values of differential settlement in different positions. The minimum radius of curvature is calculated by the fit curve of differential settlement. After that, the joint opening is calculated by the minimum radius of curvature. The fitting result is that the minimum radius of curvature is $\rho = 15.3$ km.

The horizontal opening of joint at the maximum radius of curvature of longitudinal settlement is calculated. Next relation is used to calculate the joint opening of immersed tube [11]:

$$\Delta x = \frac{Lh}{2\rho}, \tag{9}$$

where L is the length of a single segment. h is the depth of tunnel and Δx is the horizontal opening of joint. After calculation, the minimum radius of curvature of tunnel caused by differential settlement is 15.3 km. The segment joint opening is 32.7 mm.

4.4.3. Analysis of joint Since the deformability of GINA water-stop cannot be greater than the maximum allowable axial displacement of joint, which is 54.3 mm, provided by the tunnel official. It is concluded that the segment joint opening under a Grade-6 nuclear explosion, 32.7 mm, is not greater than the maximum allowable displacement.

So with the protective doors, even under Grade-6 nuclear explosion, the safety of the immersed tube structure is still guaranteed.

5. Conclusion

The damage effect of internal nuclear explosive shock wave on the main structure of cross-river tunnel. Without protective doors, under a Grade-6 air defense load, the right wall of left channel, left wall of right channel and left and right walls of middle channel do not meet the requirements for flexural capacity. While with protective doors, they all meet the requirements.

For the longitudinal structure of an immersed tube tunnel, under a Grade-6 nuclear explosive load, with protective doors, at the minimum radius of curvature of tunnel caused by differential settlement, the segment joint opening satisfies the allowable displacement of water-stop.

The impact of an indirect hit of conventional weapon on the main structure of tunnel is smaller than that of nuclear explosive shock wave.

With protective doors, nuclear explosion resistance of the immersed tube structure can be significantly increased.

References

[1] H. N. Dhakal, Z. Y. Zhang, N. Bennett, A. Lopez-Arraiza, F. J. Vallejo: *Effects of water immersion ageing on the mechanical properties of flax and jute fibre biocomposites evaluated by nanoindentation and flexural testing* . Journal of Composite Materials *48* (2014), No. 11, 1399–1406.

[2] Ayşe Öndürücü: *The effects of seawater immersion on the bearing strength of woven-glass–epoxy prepreg pin-loaded joints.* International Journal of Damage Mechanics *21* (2012), No. 2, 153–170.

[3] H. Gao, D. Carrick, C. Berry, B. E. Griffith, X. Luo: *Dynamic finite-strain modelling of the human left ventricle in health and disease using an immersed boundary-finite element method.* IMA Journal of Applied Mathematics *79* (2014), No. 5, 978–1010.

[4] S. Djili, F. Benmeddour, E. Moulin, J. Assaad, F. Boubenider: *Notch detection in copper tubes immersed in water by leaky compressional guided waves.* NDT & E International *54* (2013), 183–188.

[5] M. K. P. Kumar, K. S. Soorambail, S. B. Harisingh, A. D'costa, C. R. Chandra: *The effect of gamma radiation on the common carp (Cyprinus carpio): In vivo genotoxicity assessment with the micronucleus and comet assays.* Mutation Research/Genetic Toxicology and Environmental Mutagenesis *792* (2015), 19–25.

[6] Y. Zhu, S. Xiao, Y. Shi, Y. Yanga, Y. Wu: *A trilayer poly(vinylidene fluoride)/polyborate/poly(vinylidene fluoride) gel polymer electrolyte with good performance for lithium ion batteries.* Journal of Materials Chemistry A *1* (2013) 7790–7797.

[7] E. Lauer, X. Y. Hu, S. Hickel, N. A. Adams: *Numerical modelling and investigation of symmetric and asymmetric cavitation bubble dynamics.* Computers & Fluids *69* (2012), 1–19.

[8] A. M. A. Attia, A. R. Kulchitskiy: *Influence of the structure of water-in-fuel emulsion on diesel engine performance.* Fuel *116* (2014), 703–708.

[9] J. Tougaard, A. J. Wright, P. T. Madsen: *Cetacean noise criteria revisited in the light of proposed exposure limits for harbour porpoises.* Marine Pollution Bulletin *90* (2015), Nos. 1–2, 196–208.

[10] S. Pan, A. K. Kota, J. M. Mabry, A. Tuteja: *Superomniphobic surfaces for effec-*

tive chemical shielding. Journal of the American Chemical Society *135*, (2013), No. 2, 578–581.

[11] O. Antonov, L. Gilburd, S. Efimov, G. Bazalitski, V. Tz. Gurovich, Ya. E. Krasik: *Generation of extreme state of water by spherical wire array underwater electrical explosion*. AIP Physics of Plasmas *19* (2012), No. 10, paper 102702.

Received April 23, 2017